Communication

Improving Photocatalysis for the Reduction of CO through non-Covalent Supramolecular Assembly

Po Ling Cheung, Savannah C. Kapper, Tian Zeng, Mark E. Thompson, and Clifford P. Kubiak

J. Am. Chem. Soc., **Just Accepted Manuscript** • Publication Date (Web): 06 Sep 2019

Improving Photocatalysis for the Reduction of CO_2 Through Non-Covalent Supramolecular Assembly

Po Ling Cheung[†], Savannah C. Kapper[‡], Tian Zeng[†⊥], Mark E. Thompson[‡], Clifford P. Kubiak[†]*

[†] Department of Chemistry and Biochemistry, University of California, San Diego, 9500 Gilman Drive, La Jolla, California 92093-0358, United States

[‡] Department of Chemistry, University of Southern California, Los Angeles, California 90089, United States

Supporting Information Placeholder

ABSTRACT: We report the enhancement of photocatalytic performance by introduction of hydrogen bonding interactions to a Re bipyridine catalyst and Ru photosensitizer system (ReDAC/RuDAC) by the addition of amide substituents, with carbon monoxide (CO) and carbonate/bicarbonate as products. This system demonstrates a more-than-threefold increase in turnover number (TON_{CO} = 100 ± 4) and quantum yield (Φ_{CO} = 23.3 ± 0.8 %) for CO formation compared to the control system using unsubstituted Ru photosensitizer (RuBPY) and ReDAC (TON_{CO} = 28 ± 4 and Φ_{CO} = 7 ± 1 %) in acetonitrile (MeCN) with 1,3-dimethyl-2-phenyl-2,3-dihydro-1H-benzo[d]imidazole (BIH) as sacrificial reductant. In dimethylformamide (DMF), a solvent that disrupts hydrogen bonds, the ReDAC/RuDAC system showed a decrease in catalytic performance while the control system exhibited an increase, indicating the role of hydrogen bonding in enhancing the photocatalysis for CO_2 reduction through supramolecular assembly. The similar properties of RuDAC and RuBPY demonstrated in lifetime measurements, spectroscopic analysis, electrochemical and spectroelectrochemical studies revealed that the enhancement in photocatalysis is not due to differences in intrinsic properties of the catalyst or photosensitizer, but to hydrogen bonding interactions between them.

The efficient storage of solar energy into liquid fuels is a major challenge of renewable energy today. To mimic natural photosynthesis, photocatalytic reduction of CO_2 has been extensively investigated using transition metal complexes that can act as redox photosensitizers (PS) by transferring electrons upon photon excitation and as catalysts (Cat) by accepting electrons and reducing CO_2. Re bipyridine catalysts have been shown to be excellent electrocatalysts[1-3] and photocatalysts[4, 5] when coupled with photosensitizers. Since 2005, the Ishitani group has studied extensively supramolecular photocatalysts by linking different photosensitizers and Re catalysts using short, covalent bridging ligands[6-14]. The catalytic performance of these systems is greatly improved compared to the separated systems due to the acceleration and higher yield of intramolecular electron transfer between the two components, with the rate of electron transfer as fast as $k_{ET} = (1.4 \pm 0.1) \times 10^9\ s^{-1}$ [7]. Recently, our laboratory estimated that the rates of electron transfer (k_{ET}) between Ru_3O clusters linked by hydrogen bonded pyrimidinones were on the order of $10^{11}\ s^{-1}$ [15]. There are several reports of the influence of second coordination sphere effects, such as hydrogen bonding interactions, on catalysis[16-19]. Consequently, in this work, we investigate a bimolecular system, in which the photosensitizer and the catalyst form hydrogen bonding pairs, to determine the effects of non-covalent interactions on photocatalytic performance.

The system composed of $Ru(dac)(bpy)_2(PF_6)_2$ (RuDAC) (4,4'-bis(methyl acetamidomethyl)-2,2'-bipyridine = dac, 2,2'-bipyridine = bpy) as the photosensitizer and $Re(dac)(CO)_3Cl$ (ReDAC) as the catalyst was chosen for this study (Figure 1). A previous electrochemical study of ReDAC indicated the formation of a hydrogen-bonded Re−Re dimer in acetonitrile (MeCN)[20]. In order to fairly assess the effects of hydrogen bonding interactions on photocatalysis, a control system composed of $Ru(bpy)_3(PF_6)_2$ (RuBPY) and ReDAC was used for comparison (Figure 1). RuBPY has similar reduction potentials, UV-vis absorption spectrum, and excited state lifetime as RuDAC.

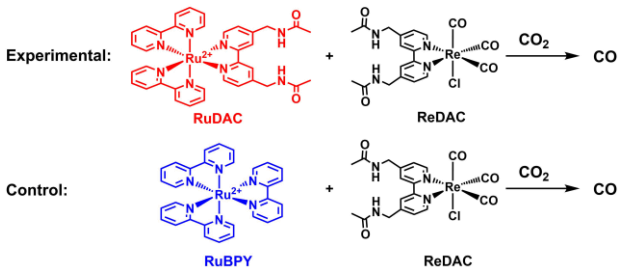

Scheme 1. Experimental and control systems for investigation of hydrogen bonding effects on photocatalysis.

ReDAC[20] and BIH[21] were synthesized as reported and RuDAC was synthesized by adapting methods in the literature[22]. In a typical mixed system with the Ru photosensitizer and catalyst as separate components, the Ru photosensitizer (Ru^{2+}) is first excited by light and then reduced by a sacrificial reductant (D), followed by electron transfer from the singly reduced Ru photosensitizer ($Ru^{\bullet+}$) to the catalyst[23, 24](Scheme 2). The latter step (eq. 2 in Scheme 2) is driven by the difference between the redox potential of $Ru^{\bullet+}$ and catalyst. To better demonstrate the impact of hydrogen bonding on photocatalysis, the first reduction potential of the photosensitizer should be comparable to that of the catalyst so that there is a low driving force for electron transfer. In the previous study, ReDAC was reported to display its first reduction at −1.77 V (vs. $Fc^{+/0}$)[20]. Cyclic voltammograms (CVs) of RuDAC, RuBPY and $Ru(dmb)_3(PF_6)_2$ (RuDMB, where 4,4'-dimethyl-2,2'-bipyridine = dmb) were taken under Ar in dry MeCN solutions containing 0.1 M tetrabutylammonium hexafluorophosphate ($TBAPF_6$). Within experimental error, the CVs of RuDAC and RuBPY display first

reduction potentials at −1.76 V, making them excellent trial systems comparing hydrogen bonding effects in this study. Another commonly used photosensitizer, RuDMB, has a more negative reduction potential at −1.88 V. The increased driving force for electron transfer could mask hydrogen bonding effects. Therefore, RuBPY was chosen to be the control for comparison of catalytic performance without a hydrogen bonding interaction.

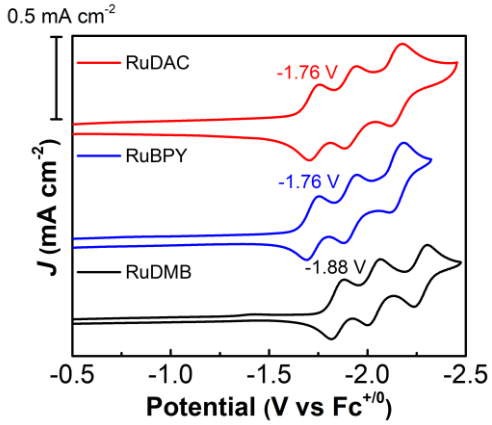

Figure 1. Cyclic voltammograms of 1 mM of RuDAC (red), RuBPY (blue) and RuDMB (black) in dry MeCN containing 0.1 M $TBAPF_6$ at scan rate 100 mV/s under Ar.

$$Ru^{2+*} + D \longrightarrow Ru^{+} + D^{+} \quad (1)$$

$$Ru^{+} + Cat \longrightarrow Cat^{-} + Ru^{2+} \quad (2)$$

Scheme 2. A simplified scheme showing reductive quenching of the Ru photosensitizer (Ru) by sacrificial reductant (D) and then the electron transfer from singly reduced Ru to the catalyst (Cat).

A series of photocatalytic studies were performed by irradiating solutions that were 0.5 mM in photosensitizer, 0.5 mM in catalyst, 0.1 M in 1,3-dimethyl-2-phenyl-2,3-dihydro-1H-benzo[d]imidazole (BIH) in dry MeCN or *N*,*N*-dimethylformamide (DMF) under CO_2 or Ar at 470 nm for 4 h. The common practice of using triethanolamine (TEOA) as proton source and 1-benzyl-1,4-dihydronicotinamide (BNAH) as sacrificial reductant was not adopted in this study as these have hydroxyl or amide groups which are capable of interrupting the hydrogen bonding between the photosensitizer and the catalyst. The systems in this study work surprisingly well without the added proton source, and it is likely due to the disproportionation mechanism of $2CO_2 + 2e^-$ to CO and CO_3^{2-} or HCO_3^- ($[H]CO_3^{[2]-}$) by the ReDAC catalyst[20]. In MeCN solutions, hydrogen bonds can be formed between amide substituents as demonstrated in previous electrochemical studies of ReDAC[20]. The photocatalytic reactions were run for 4 hours only because over half of the BIH was consumed. After 4 hours of irradiation, the RuDAC/ReDAC system exhibits a more-than-threefold increase in photocatalytic reduction of CO_2 with a higher turnover number (TON_{CO} = 100 ± 4) and quantum yield (Φ_{CO} = 23.3 ± 0.8 %) for CO production compared to the RuBPY/ReDAC control system (TON_{CO} = 28 ± 4 and Φ_{CO} = 7 ± 1 %) as shown in Figure 2. To further test hydrogen bonding as the principal cause for these observations, similar photocatalytic studies were done in DMF, a solvent that interrupts hydrogen bond formation. In DMF (Figure 2), the RuBPY/ReDAC control system displays improvement in catalysis (TON_{CO} = 43 ± 9 and Φ_{CO} = 11 ± 1 %) while the RuDAC/ReDAC system displays a decrease in catalysis (TON_{CO} = 79 ± 8 and Φ_{CO} = 18 ± 1 %), but it still outperforms the RuBPY/ReDAC system. Thus, the two systems exhibit opposite responses to different solvents. The higher activity of the RuDAC/ReDAC system compared to the control system in DMF is unexpected, but it is likely due to increased contact surface area between photosensitizer and catalyst[25]. The reason for higher activity of RuBPY/ReDAC in DMF compared to MeCN remains unclear, but previous studies show that solvents play important roles in controlling catalytic rates and selectivity[23, 26-30]. Since the RuDAC/ReDAC system behaves in a trend opposite to the control, it is reasonable to conclude that hydrogen bonding is the dominant factor influencing differences in performance.

In addition to gaseous products, the liquid mixtures were analyzed. No formate is detected with ^1H NMR (Table S1 and S2) but appreciable $[H]CO_3^{[2]-}$ are observed with IR. It is known that ReDAC undergoes the disproportionation mechanism of $2CO_2 + 2e^- \leftrightharpoons CO$ and CO_3^{2-} in electrocatalysis[20]. When a proton source is not used in the photocatalytic experiments, bands are observed in the IR at 1672 and 1637 cm^{-1}, consistent with formation of $[H]CO_3^{[2]-}$ species (Figure S5). Repeating these experiments with $^{13}CO_2$ showed shifts in these bands (1625 and 1598 cm^{-1}), consistent with isotopic labeling[20, 31]. Control studies under Ar reveal no CO or H_2 production upon irradiation (Table S2). In addition, control reactions without ReDAC reveal that RuDAC is a better catalyst than RuBPY in both solvents and it performed better in MeCN than in DMF. These observations are similar to the trend seen in the RuDAC/ReDAC system, but the absence of the Re catalyst significantly slows down the rate of CO formation (Table S2).

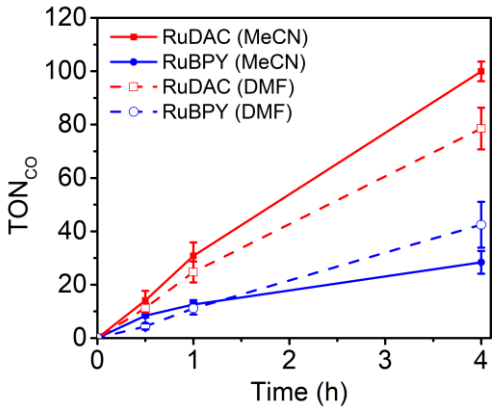

Figure 2. Turnover number of CO (TON_{CO}) produced by RuDAC/ReDAC (red) and RuBPY/ReDAC (blue) in MeCN (solid line) and DMF (dotted line) solvents.

Several additional experiments were carried out to understand the origin of the enhancement in photocatalytic activity in the RuDAC/ReDAC system compared to RuBPY/ReDAC. Further support for hydrogen bonding interactions was gained as contributions arising from discrepancies in light absorption by the photosensitizers, faster electron transfer from BIH to the photosensitizer, and other interactions of the photosensitizer with the catalyst were ruled out. First, the photochemical properties of the photosensitizers were investigated. The UV-visible absorption measurements of the three photosensitizers show comparable molar absorptivity at 470 nm, which is the wavelength used for photocatalysis (Table 1 and Figure S3). The lifetimes of the excited states were measured by Time−Correlated Single Photon Counting (TCSPC) with excitation wavelength at 405 nm at room temperature. The lifetimes of excited RuDAC were found to be 980 ns and 910 ns in MeCN and DMF respectively (Table 1 and Fig. S6). Since there is a range of values for the reported lifetimes of RuBPY[32] and RuDMB[13, 33], we measured them in this work for consistency (Table 1). The photoinduced

Table 1. Photochemical properties of RuDAC, RuBPY and RuDMB.

complex	$\lambda_{em\ (MeCN)}$ (nm) [a]	$\lambda_{em\ (DMF)}$ (nm) [a]	ε_{470}(L mol^{-1} cm^{-1})	τ_{MeCN} (ns) [b]	τ_{DMF} (ns) [b]	$\kappa_{q\ (MeCN)}$ (M^{-1} s^{-1}) [c]	$\kappa_{q\ (DMF)}$ (M^{-1} s^{-1}) [c]
RuDAC	613	620	7200	980	910	$5.9 \pm 0.2 \times 10^9$	$1.8 \pm 0.2 \times 10^9$
RuBPY	609	618	9000	930	930	$7.2 \pm 0.2 \times 10^9$	$2.6 \pm 0.2 \times 10^9$
RuDMB	618	624	8100	900	790		

[a] A dry MeCN or DMF solution containing the Ru complex was measured using fluorometer. [b] The fluorescence lifetimes were measured in dry MeCN or DMF using TCSPC with excitation wavelength at 405 nm at room temperature. [c] The quenching constants were obtained by the Stern−Volmer plot of reductive quenching with BIH in dry MeCN or DMF (Fig. S7 and S8)

electron transfer from BIH to Ru photosensitizers is the initial process in the photocatalytic CO_2 reduction[34]. To determine the rate of this process, the quenching constant (k_q) was found by fluorescence lifetime measurements and the following equation[35]:

$$\frac{\tau_0}{\tau} = 1 + \tau_0 \kappa_q [Q] = 1 + K_D[\mathrm{Q}] \quad (1)$$

Here, τ_0 and τ are the fluorescence lifetimes without and with the quencher respectively, k_q is the biomolecular quenching constant, K_D is the Stern−Volmer constant for dynamic quenching, and Q is the quencher. By plotting the Stern−Volmer relationship (Fig. S7 and S8), the slope was used to calculate the quenching rate constant (k_q) using eq. 1. The non-zero slope from the plots suggests dynamic quenching between BIH and the Ru photosensitizers. While the quenching rates of RuDAC and RuBPY are comparable to each other in MeCN and DMF respectively, the rates in MeCN are two to three times higher than those in DMF, indicating a faster electron transfer process in MeCN (Table 1).

Further electrochemical studies were carried out to examine the interaction between photosensitizer and catalyst. RuDAC has three quasi-reversible reduction peaks at −1.76 V, −1.52 V and −2.18 V in MeCN and DMF (Figure S11 and S12) respectively. Similar to other Ru bipyridine complexes[36], RuDAC itself exhibits current enhancement under a CO_2 atmosphere in both solvent systems (Figure S9 and S10). Addition of ReDAC to the cell causes no significant changes to the three reversible reductions of RuDAC. However, as revealed in the CV of RuDAC/ReDAC in MeCN under CO_2 (Figure S13), the characteristic catalytic peak at around -1.8 V vs. $Fc^{+/0}$ is similar to ReDAC alone in MeCN[20], suggesting the formation of the ReDAC dimer. This indicates that the presence of RuDAC does not interfere in the catalytic reaction of ReDAC. The absence of the ReDAC hydrogen bonded dimer feature in the CV under catalytic conditions in DMF (Figure S14) also provides clear evidence that DMF disrupts hydrogen bonding[20]. To further test this hypothesis, IR spectroelectrochemistry (IR-SEC) studies were conducted on the RuDAC/ReDAC system in MeCN under N_2. The IR spectra of Figure S15 indicate the formation of the Re−Re dimer from ReDAC as reported in a previous electrochemical study[20], indicating that RuDAC is unlikely to affect the catalytic mechanism of ReDAC. Using NMR concentration studies, we estimate the association constant (K_a) for the hetero-dimer of [ReDAC···RuDAC] to be approximately 300 M^{-1} in MeCN (Figure S16)[37], which is close to the self-dimerization constant of ReDAC[20]. Although an approximately statistical mixture of homo- and hetero-dimers is expected in the RuDAC/ReDAC system, the hydrogen bonding interaction is strong enough to boost catalysis significantly.

In conclusion, the findings reported here taken together demonstrate that appending amide groups to photosensitizer and catalyst significantly improves photocatalysis in MeCN by enabling hydrogen bonding interactions. To the best of our knowledge, this constitutes the first report of successfully utilizing hydrogen bonding groups on photosensitizers and catalysts to improve photocatalytic CO_2 reduction. A forthcoming study will employ specific hydrogen bond donor and acceptors on photosensitizers and catalysts to eliminate self-dimerization effects.

ASSOCIATED CONTENT

Supporting Information

The Supporting Information is available free of charge on the ACS Publications website.

Experimental details and additional NMR, mass spectrum, TCSPC traces, Stern−Volmer plots, UV-vis spectrum, infrared, electrochemical and photochemical studies and IR-SEC.

AUTHOR INFORMATION

Corresponding Author

* ckubiak@ucsd.edu

ORCID

Po Ling Cheung: 0000-0002-2717-0339
Mark E. Thompson: 0000-0002-7764-4096
Clifford P. Kubiak: 0000-0003-2186-488X

Present Addresses

⊥ Division of Chemistry and Chemical Engineering, California Institute of Technology, Pasadena, California 91125, United States

Notes

The authors declare no competing financial interests.

ACKNOWLEDGMENT

This project was supported by two funding sources. A grant from the Air Force Office of Scientific Research (AFOSR), Basic Research Initiative (BRI) grant (FA9550-12-1-0414), supported Cheung, Zeng, and Kubiak, whose work involved synthesis and characterization of all compounds, photocatalytic studies, electrochemical studies, IR-SEC studies, NMR studies, fluorescence measurements and data analysis. The Office of Basic Energy Sciences at the Department of Energy (DE-SC0016450) supported Kapper and Thompson, whose work involved TCSPC measurements, fluorescence measurements, and data analysis.

REFERENCES

1. Clark, M. L.; Cheung, P. L.; Lessio, M.; Carter, E. A.; Kubiak, C. P., Kinetic and Mechanistic Effects of Bipyridine (bpy) Substituent, Labile Ligand, and Brønsted Acid on Electrocatalytic CO_2 Reduction by Re(bpy) Complexes. *ACS Catal.* **2018,** *8* (3), 2021-2029.
2. Hawecker, J.; Lehn, J. M.; Ziessel, R., Electrocatalytic reduction of carbon dioxide mediated by $Re(bipy)(CO)_3Cl$ (bipy = 2,2′-bipyridine). *J. Chem. Soc., Chem. Commun.* **1984**, 328-330.
3. Hawecker, J.; Lehn, J. M.; Ziessel, R., Photochemical and Electrochemical Reduction of Carbon Dioxide to Carbon Monoxide Mediated by (2,2′-Bipyridine)tricarbonylchlororhenium(I) and Related Complexes as Homogeneous Catalysts. *Helv. Chim. Acta* **1990,** *69*, 1990-2013.

4. Koike, K.; Hori, H.; Ishizuka, M.; Westwell, J. R.; Takeuchi, K.; Ibusuki, T.; Enjouji, K.; Konno, H.; Sakamoto, K.; Ishitani, O., Key Process of the Photocatalytic Reduction of CO_2 Using [Re(4,4'-X_2-bipyridine)$(CO)_3PR_3$]+ (X = CH_3, H, CF_3; PR_3 = Phosphorus Ligands): Dark Reaction of the One-Electron-Reduced Complexes with CO_2. *Organometallics* **1997,** *16*, 5724-5729.
5. Agarwal, J.; Fujita, E.; Schaefer, H. F.; Muckerman, J. T., Mechanisms for CO Production from CO_2 Using Reduced Rhenium Tricarbonyl Catalysts. *J. Am. Chem. Soc.* **2012,** *134*, 5180–5186.
6. Kamata, R.; Kumagai, H.; Yamazaki, Y.; Sahara, G.; Ishitani, O., Photoelectrochemical CO_2 Reduction Using a Ru(II)-Re(I) Supramolecular Photocatalyst Connected to a Vinyl Polymer on a NiO Electrode. *ACS Appl. Mater. Interfaces* **2019,** *11* (6), 5632-5641.
7. Koike, K.; Grills, D. C.; Tamaki, Y.; Fujita, E.; Okubo, K.; Yamazaki, Y.; Saigo, M.; Mukuta, T.; Onda, K.; Ishitani, O., Investigation of excited state, reductive quenching, and intramolecular electron transfer of Ru(II)-Re(I) supramolecular photocatalysts for CO_2 reduction using time-resolved IR measurements. *Chem. Sci.* **2018,** *9*, 2961-2974.
8. Kumagai, H.; Sahara, G.; Maeda, K.; Higashi, M.; Abe, R.; Ishitani, O., Hybrid Photocathode Consisting of $CuGaO_2$ *p*-Type Semiconductor and a Ru(II)-Re(I) Supramolecular Photocatalyst: Non-Biased Visible-Light-Driven CO_2 Reduction with Water Oxidation. *Chem. Sci.* **2017,** *8*, 4242-4249.
9. Kuramochi, Y.; Ishitani, O., Iridium(III) 1-Phenylisoquinoline Complexes as a Photosensitizer for Photocatalytic CO_2 Reduction: A Mixed System with a Re(I) Catalyst and a Supramolecular Photocatalyst. *Inorg. Chem.* **2016,** *55*, 5702-5709.
10. Sato, S.; Koike, K.; Inoue, H.; Ishitani, O., Highly efficient supramolecular photocatalysts for CO_2 reduction using visible light. *Photochem. Photobiol. Sci.* **2007,** *6* (4), 454-61.
11. Tamaki, Y.; Ishitani, O., Supramolecular Photocatalysts for the Reduction of CO_2. *ACS Catal.* **2017,** *7* (5), 3394-3409.
12. Tamaki, Y.; Koike, K.; Morimoto, T.; Yamazaki, Y.; Ishitani, O., Red-Light-Driven Photocatalytic Reduction of CO_2 using Os(II)-Re(I) Supramolecular Complexes. *Inorg. Chem.* **2013,** *52*, 11902-11909.
13. Tamaki, Y.; Watanabe, K.; Koike, K.; Inoue, H.; Morimoto, T.; Ishitani, O., Development of highly efficient supramolecular CO_2 reduction photocatalysts with high turnover frequency and durability. *Faraday Discuss.* **2012,** *155*, 115-127.
14. Ueda, Y.; Takeda, H.; Yui, T.; Koike, K.; Goto, Y.; Inagaki, S.; Ishitani, O., A Visible-Light Harvesting System for Efficient CO_2 Reduction Using a Supramolecular Ru(II)-Re(I) Photocatalyst Adsorbed in Periodic Mesoporous Organosilica. *ChemSusChem* **2015,** *8*, 439-442.
15. Porter, T. M.; Heim, G. P.; Kubiak, C. P., Stable Mixed-Valent Complexes Formed by Electron Delocalization Across Hydrogen Bonds of Pyrimidinone-Linked Metal Clusters. *J. Am. Chem. Soc.* **2018,** *140* (40), 12756-12759.
16. Sahu, S.; Cheung, P. L.; Machan, C. W.; Chabolla, S. A.; Kubiak, C. P.; Gianneschi, N. C., Charged Macromolecular Rhenium Bipyridine Catalysts with Tunable CO_2 Reduction Potentials. *Chem. Eur. J.* **2017,** *23*, 8619-8622.
17. Azcarate, I.; Costentin, C.; Robert, M.; Savéant, J.-M., Through-Space Charge Interaction Substituent Effects in Molecular Catalysis Leading to the Design of the Most Efficient Catalyst of CO_2-to-CO Electrochemical Conversion. *J. Am. Chem. Soc.* **2016,** *138*, 16639–16644.
18. Doud, M. D.; Grice, K. A.; Lilio, A. M.; Seu, C. S.; Kubiak, C. P., Versatile Synthesis of $PR_2NR'_2$ Ligands for Molecular Electrocatalysts with Pendant Bases in the Second Coordination Sphere. *Organometallics* **2012,** *31*, 779-782.
19. Bays, J. T.; Priyadarshani, N.; Jeletic, M. S.; Hulley, E. B.; Miller, D. L.; Linehan, J. C.; Shaw, W. J., The Influence of the Second and Outer Coordination Spheres on Rh(diphosphine)$_2$ CO_2 Hydrogenation Catalysts. *ACS Catal.* **2014,** *4*, 3663-3670.
20. Machan, C. W.; Chabolla, S. A.; Yin, J.; Gilson, M. K.; Tezcan, F. A.; Kubiak, C. P., Supramolecular assembly promotes the electrocatalytic reduction of carbon dioxide by Re(I) bipyridine catalysts at a lower overpotential. *J. Am. Chem. Soc.* **2014,** *136* (41), 14598-607.
21. Hong, D.; Tsukakoshi, Y.; Kotani, H.; Ishizuka, T.; Kojima, T., Visible-Light-Driven Photocatalytic CO_2 Reduction by a Ni(II) Complex Bearing a Bioinspired Tetradentate Ligand for Selective CO Production. *J. Am. Chem. Soc.* **2017,** *139* (19), 6538-6541.
22. Aranyos, V.; Hagfeldt, A.; Grennberg, H.; Figgemeier, E., Electropolymerisable bipyridine ruthenium(II) complexes: synthesis, spectroscopic and electrochemical characterisation of 4-((2-thienyl) ethenyl)- and 4,4′-di((2-thienyl) ethenyl)-2,2′-bipyridine ruthenium complexes. *Polyhedron* **2004,** *23* (4), 589-598.
23. Cheung, P. L.; Machan, C. W.; Malkhasian, A. Y.; Agarwal, J.; Kubiak, C. P., Photocatalytic Reduction of Carbon Dioxide to CO and HCO_2H Using *fac*-Mn(CN)(bpy)$(CO)_3$. *Inorg. Chem.* **2016,** *55* (6), 3192-8.
24. Yamazaki, Y.; Takeda, H.; Ishitani, O., Photocatalytic reduction of CO_2 using metal complexes. *J. Photochem. Photobiol. C: Photochem. Rev.* **2015,** *25*, 106-137.
25. Porter, T. M.; Canzi, G. C.; Chabolla, S. A.; Kubiak, C. P., Tuning Electron Delocalization and Transfer Rates in Mixed-Valent Ru_3O Complexes through "Push–Pull" Effects. *J. Phys. Chem. A* **2016,** *120* (32), 6309-6316.
26. Takeda, H.; Kamiyama, H.; Okamoto, K.; Irimajiri, M.; Mizutani, T.; Koike, K.; Sekine, A.; Ishitani, O., Highly Efficient and Robust Photocatalytic Systems for CO_2 Reduction Consisting of a Cu(I) Photosensitiser and Mn(I) Catalysts. *J. Am. Chem. Soc.* **2018,** *140*, 17241-17254.
27. Morimoto, T.; Nakajima, T.; Sawa, S.; Nakanishi, R.; Imori, D.; Ishitani, O., CO_2 capture by a rhenium(I) complex with the aid of triethanolamine. *J. Am. Chem. Soc.* **2013,** *135* (45), 16825-8.
28. Paul, A.; Connolly, D.; Schulz, M.; Pryce, M. T.; Vos, J. G., Effect of Water during the Quantitation of Formate in Photocatalytic Studies on CO_2 Reduction in Dimethylformamide. *Inorg. Chem.* **2012,** *51*, 1977–1979.
29. Kuramochi, Y.; Kamiya, M.; Ishida, H., Photocatalytic CO_2 Reduction in *N*,*N*-Dimethylacetamide/Water as an Alternative Solvent System. *Inorg. Chem.* **2014,** *53*, 3326–3332.
30. Lee, S. K.; Kondo, M.; Okamura, M.; Enomoto, T.; Nakamura, G.; Masaoka, S., Function-Integrated Ru Catalyst for Photochemical CO_2 Reduction. *J. Am. Chem. Soc.* **2018,** *140* (49), 16899-16903.
31. Sampson, M. D.; Kubiak, C. P., Manganese Electrocatalysts with Bulky Bipyridine Ligands: Utilizing Lewis Acids To Promote Carbon Dioxide Reduction at Low Overpotentials. *J. Am. Chem. Soc.* **2016,** *138* (4), 1386-1393.
32. Arias-Rotondo, D. M.; McCusker, J. K., The photophysics of photoredox catalysis: a roadmap for catalyst design. *Chem. Soc. Rev.* **2016,** *45* (21), 5803-5820.
33. Kato, E.; Takeda, H.; Koike, K.; Ohkuboa, K.; Ishitani, O., Ru(II)–Re(I) binuclear photocatalysts connected by –CH_2XCH_2– (X = O, S, CH_2) for CO_2 reduction. *Chem. Sci.* **2015,** *6*, 3003-3012.
34. Kuramochi, Y.; Ishitani, O.; Ishida, H., Reaction mechanisms of catalytic photochemical CO_2 reduction using Re(I) and Ru(II) complexes. *Coord. Chem. Rev.* **2018,** *373*, 333-356.
35. Fraiji, L. K.; Hayes, D. M.; Werner, T. C., Static and dynamic fluorescence quenching experiments for the physical chemistry laboratory. *J. Chem. Educ.* **1992,** *69*, 424-428.
36. Ishida, H.; Tanaka, K.; Tanaka, T., Electrochemical CO_2 reduction catalyzed by ruthenium complexes $[Ru(bpy)_2(CO)_2]^{2+}$ and $[Ru(bpy)_2(CO)Cl]^+$. Effect of pH on the formation of CO and $HCOO^-$. *Organometallics* **1987,** *6* (1), 181-186.
37. Hynes, M. J., EQNMR: A computer program for the calculation of stability constants from nuclear magnetic resonance chemical shift data. *J. Chem. Soc., Dalton Trans.* **1993**, 311-312.

Insert Table of Contents artwork here